Journal of Nanoparticle Research **4:** 395–403, 2002.

Imaging {Au^0-PAMAM} gold-dendrimer nanocomposites in cells

Anna Bielinska, Jonathan D. Eichman, Inhan Lee, James R. Baker, Jr. and Lajos Balogh*
*Center for Biologic Nanotechnology, University of Michigan, 4010 Kresge Research Building II, 200 Zina Pitcher Place, Ann Arbor, MI 48109-0533, USA; *Author for correspondence (Tel.: (734)615-0623; Fax: (734)615-0621; E-mail: baloghl@umich.edu)*

Received 26 January 2002; accepted in revised form 14 August 2002

Key words: nanocomposites, dendrimers, imaging, gene transfer, drug delivery, gold/dendrimer composite

Abstract

Dendrimer nanocomposites (DNC) are hybrid nanoparticles formed by the dispersion and immobilization of guest atoms or small clusters in dendritic polymer matrices. They have a great potential in biomedical applications due to their controlled composition, predetermined size, shape and variable surface functionalities. In this work, $d = 5$–25 nm spherical nanoparticles composed of gold and poly(amidoamine) (PAMAM) dendrimers have been selected to demonstrate this nanoparticle based concept. {$Au(0)_n$-PAMAM} gold dendrimer nanocomposites with a well-defined size were synthesized and imaged by transmission electron microscopy both *in vitro* and *in vivo*. DNC have also the potential to be used for imaging and drug delivery vehicles either by utilizing bioactive guests or through the incorporation of radioactive isotopes, such as Au-198.

Introduction

Poly(amidoamine) (PAMAM) dendrimers contain beta-alanine repeat units thus can be viewed as spherical artificial proteins that may be used as building blocks of nanoscopic devices. However, PAMAM dendrimers are aliphatic, therefore they are extremely difficult to observe directly in cells or in tissue. Generally, the attachment of fluorescent markers, radioactive substituents or surface complexes of metal ions, such as Gd^{3+}, are used to overcome this obstacle. A shortcoming of this method is that conjugation of markers to the surface of a PAMAM may dramatically change the solubility of the macromolecule and alter other surface-related properties. This problem can readily be solved by using dendrimer nanocomposites (DNC) that can be composed of different materials. Monodisperse dendrimer nanocomposites can be synthesized in various predetermined sizes and their interaction with biological objects may be adjusted by modifying their surface properties. They readily penetrate into cells and are easy to observe by transmission electron microscopy (TEM) and optical methods.

Dendrimers

Dendrimers are monodisperse symmetric macromolecules containing connectors and branching units built around a small molecule or a linear polymer core (Tomalia et al., 1984; 1985; Newkome et al., 1985; Hawker et al., 1990). The high level of synthetic control allows the synthesis of a narrow molecular weight range of well-defined and highly symmetrical polymer molecules, which contain a large number of regularly spaced internal and external functional groups. As a result, the interior of a dendrimer may be hydrophilic while its exterior is hydrophobic, or vice versa, depending on the design and synthesis.

Interaction of dendrimer macromolecules with the molecular environment is controlled dominantly by their surface groups. In case of high generation (>6 in the case of PAMAM) dendrimers that are dense-packed, contribution to the surface may be solely due to terminal groups. In the more open structures of lower

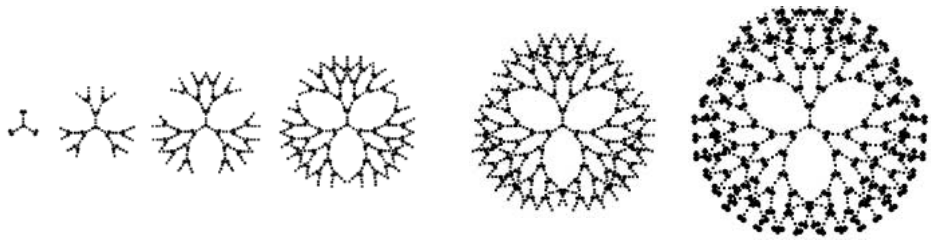

Figure 1. Structural scheme of ideal dendritic growth from a trivalent (e.g. ammonia) core up to a generation four dendrimer. In the case of a (PAMAM dendrimer, G-1 structure denotes the following molecule: $N(CH_2CH_2CONHCH_2CH_2NH_2)_3$, the connector being: $–CH_2CH_2CONHCH_2CH_2–$, (beta-alanine subunits). the branching site is –N< and the surface is $–NH_2$ (Diameter data are taken from the literature: Tomalia et al., 1990).

generations the penultimate functional groups also contribute to this interaction in an increasing fashion as the generational number decreases (Figure 1).

However, 'dendrimer' describes only an architectural motif and not a specific compound (despite the fact that this term is extensively used in the literature for branching molecules). Due to synthesis limitations dendrimer materials always contain imperfect molecules and these defective molecules are more similar to hyperbranched structures. Therefore, one must be very careful when summarizing results about 'dendritic polymers', because the results often cannot be taken out of context. Dendritic properties of a given polymer material can neither be assessed nor evaluated without taking into account the composition and the dendritic purity (rate of molecules with perfect structures to all polymer molecules present) of the actual macromolecules.

As an example, PAMAM dendrimers (Tomalia et al., 1996) undergo changes in size, shape and flexibility as a function of increasing generations (from a small branching molecule at generation zero to organic particles behaving as hard spheres at generation seven) (de Gennes & Hervert, 1983; Tomalia et al., 1990; Mansfield & Klushin, 1993; Bhalgat et al., 2000).

There are many ways to construct polymers with dendritic architecture depending on which part of the macromolecule is dendritic and what different authors consider to be a dendrimer. To date greater than 160 various dendritic structures are reported in the literature.

Composites and nanocomposites

Composites are physical mixtures or two or more organic and/or inorganic components, which display improved properties in one or more areas as compared to their individual bulk constituents. They are widely used in many diverse industries and form the basics of engineering plastics, structural adhesives and matrices. They contain at least one continuous phase and dispersed phase(s), which may have various compositions, sizes, size distributions and shape. Recent developments in materials research have shown that it is possible to achieve a nonlinear enhancement of material properties in composite systems by decreasing the size of the phase domains into the nanometer range. Nanocomposites can be defined as having at least one component with at least one dimension <100 nm. A more rigorous definition requires that all dimensions of all components <100 nm. Thus, nanocomposite properties will be strongly influenced by extensive interfacial interactions between the components and the rule of mixtures fails to provide estimates of nanocomposite properties.

Dendrimer nanocomposites

According to the general concept of dendrimer nanocomposites (Balogh et al., 1997; Beck Tan et al., 1997), small precursors to a desired product are preorganized by an appropriately selected dendrimer in the first step. This preorganization is followed by *in situ* chemical reaction(s) or physical treatment (irradiation, etc.) that generates immobilized reaction products. This procedure yields dispersed small domains of guest molecules that are integrated with the dendrimer molecule without having covalent bonds between the dendrimer and the topologically entrapped matter. Dendrimer templated nanocomposites may be constructed with flexible architectures and

in variable compositions resulting in predetermined nanostructures.

Nomenclature

To describe the complex structure of these nanoscopic complexes and nanocomposites we use the following convention to describe the composition of the synthesized nanomaterials: brackets denote complexes while braces represent nanocomposite structures. Within the brackets or braces, first the complexed or encapsulated components are listed (with an index of their average number per dendrimer molecule) then the family of dendrimers followed by terms used for dendrimer identification, i.e., core, generation and surface. Naming then would follow this pattern: $\{(\text{comp\#1})_i(\text{comp\#2})_j(\text{comp\#3})_{k...}$-FAMILY_CoreGeneration.Terminal group$\}$. Thus, the formula of $\{(Au^0)_{14}$-PAMAM_E4·$NH_2\}$ denotes a gold dendrimer nanocomposite in which a generation four amine terminated ethylenediamine (EDA or E for short) core PAMAM dendrimer contains 14 zerovalent gold atoms. The above scheme provides a relatively simple but consistent way to identify materials with a complicated structure (Figure 2). In this paper, as only PAMAM dendrimers were used, we usually followed the shorter pattern and omitted naming the dendrimer. Thus, $\{(Au(0))_{10}$-PAMAM_E5·$NH_2\}$ and $\{(Au(0))_{10}$-E5·$NH_2\}$ are considered to be equivalent names in this publication.

Gold nanocomposites

Various synthesis methods and subsequent characterization of the resulting gold-PAMAM nanocomposites are recently in the focus of interest.

Gold/PAMAM nanocomposites usually are fabricated by UV-irradiation (Esumi et al., 1998) or by chemical reduction of tetrachloroaurate salts of PAMAM dendrimers. In the two extreme cases, (depending on the reaction conditions) the dendrimers may either encapsulate the colloidal gold (Garcia et al., 1999; Esumi et al., 2000) or, alternatively, gold nanocrystals may grow in the interior of the PAMAM molecules (Gröhn et al., 2000). DNC structures most frequently are amorphous or nearly amorphous. Based on the locality of the guest atoms three different types of single nanocomposite architectures have been identified, such as internal ('I'), external ('E') and mixed ('M') type nanocomposites (Balogh et al., 1999). Structure of both $\{(Au(0))_n$-PAMAM$\}$ and $\{(Ag(0))_n$-PAMAM$\}$ gold and silver dendrimer nanocomposites was found to be the function of the dendrimer host structure and its surface groups as well as the formation mechanism and the chemistry involved (He et al., 1999) (Figure 3).

In real systems, both the organic and inorganic phase could form nano-sized pseudo-continuous phases while the other components are dispersed at the molecular or atomic level either in the interior or on the surface of the template/container. Single units of these nanocomposites may be used as building

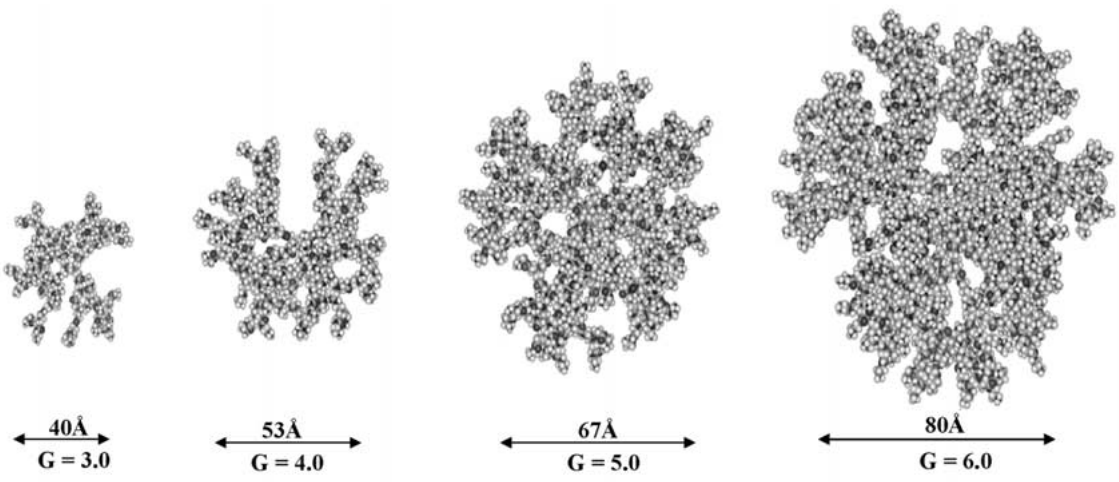

Figure 2. Size and shape of ethylenediamine core PAMAM dendrimers as a function of generation. Dendritic polymers provide a multifunctional surface with a variable size and tunable compatibility.

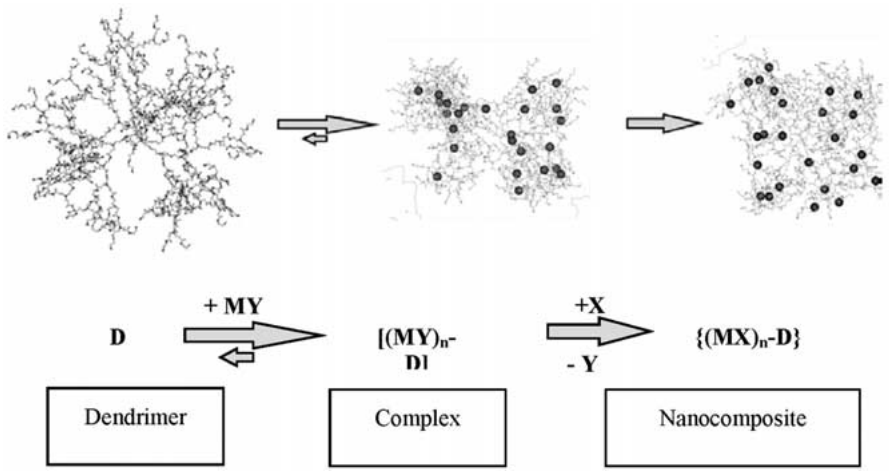

Figure 3. General scheme of dendrimer nanocomposite synthesis through a metal ion complex intermediate.

blocks in the synthesis of nanostructured materials and devices.

Examples of using PAMAM dendrimers in medicine

Imaging

PAMAM dendrimers have been used for imaging but only after appropriate surface modification. The potential of polyamidoamine metal-chelate-dendrimer-antibody constructs in radioimmunotherapy and imaging has been recognized early (Wu et al., 1994). Generally, fluorescent markers, such as fluorescein, or chelated metal ions, such as Gd^{3+} for MRI are used to generate a measurable signal (Margerum et al., 1997; Kim & Zimmerman, 1998). Radiolabeled compounds (3-H, 14-C, 125-I or 153-Gd) are also used as labels in biodistribution studies (Kobayashi et al., 2001). Surface of PAMAM dendrimers were also modified chemically by various macrocycles (Wu et al., 1994), such as *N*-[2-amino-3-(*p*-isothiocyanatophenyl)propyl]-trans-cyclohexane-1,2-diamine-*N*,*N*′,*N*′,*N*″,*N*″-pentaacetic acid, for short: *p*-SCN-Bz-CHX-B-DTPA and 2-(*p*-isothiocyanatobenzyl)-1,4,7,10-tetraazacyclododecane-*N*,*N*′,*N*″,*N*‴-tetraacetate, for short: *p*-SCN-Bz-DOTA, as metal chelators and were coupled to a monoclonal antibody without loss of protein immunoreactivity. Both the DTPA- and DOTA-dendrimer antibody constructs were easily labeled with 90-Y, 212-Bi or cold Gd(III) suggesting use of this dendrimer-macrocycle for guided radiotherapy or imaging. Nonetheless, conjugation of markers to the surface of the macromolecule may dramatically change the solubility and other surface-related properties.

Gene transfer

It has been reported that PAMAM dendrimers can be effective carriers for the introduction of various types of nucleic acids, e.g., the expression plasmids, single stranded DNA oligonucleotides or RNA. That particular function of PAMAM dendrimers relies on their ability to bind all forms of charged nucleic acids on the basis of electrostatic interactions. The resulting dendrimer/DNA complexes enhance DNA transfer, protect against intra- and extra-cellular degradation and results in the transgene expression in a variety of mammalian cell lines *in vitro* as well in variety of animal tissue *in vivo* (Bielinska et al., 1996).

Several studies have demonstrated that PAMAM dendrimers can transfect a wide variety of cell types *in vitro* and offer an efficient method for producing permanently transfected cell lines. The capability of a PAMAM dendrimer to transfect cells appeared to depend on the size, shape, and number of primary amino groups on the surface of the polymer (Kukowska-Latallo et al., 1996; Qin et al., 1998). The ability of the dendrimer to complex and form aggregates with DNA is crucial for efficient transfection and the function of the complexed DNA. Formation of DNA-dendrimer complexes seems to be based entirely on charge interaction between negatively charged phosphate groups of the nucleic acid and protonated (positively charged) amino groups of the PAMAM

polymers (Bielinska et al., 1997; Roessler et al., 2001). Highly efficient transfection of a broad range of eukaryotic cells and cell lines was achieved with minimal cytotoxicity using these DNA/dendrimer complexes. It was found that the ability of DNA-PAMAM to transfect cells can be improved in the presence of additional compounds that appeared to alter the structure the complex and/or dispersion of the population of particles (Roessler et al., 2001).

In the majority of cells the transfection can be also enhanced with the addition of chloroquine. This indicating involvement of endosomes in trafficking of the complexes.

To clarify the structure of DNA-PAMAM complex interactions of nitroxide-labeled PAMAM dendrimers (EDA core, amine terminated, generation 2 and 6, i.e., PAMAM_E2·NH_2 and PAMAM_E6·NH_2) to various DNA molecules have also been investigated by ESR (Ottaviani et al., 1999; Chen et al., 2000). The results show that although the structure of the complex depends on both the PAMAM generation and the length of the DNA strand, there is predominantly one binding mode between DNA and PAMAM dendrimers. The structure or the stoichiometric complex and various aggregates changes not only with surface charge differential but is dependent on the concentration of both components (Bielinska et al., 1996). The simplest structural model proposes that DNA binding with dendrimers can be divided into tightly bound DNA regions and linker DNA regions. The binding between DNA and dendrimers also effected by ionic strength and pH, which is consistent with the importance of the electrostatic interactions in the DNA-dendrimer binding.

Targeting and drug delivery

Targeting of tumor cells may be performed by either non-specific or specific ways as it is described in the related literature. Receptor specific targeting and optimization of surface properties are also possible. Targeting groups can be conjugated to the host dendrimer's surface (Wilbur et al., 1998) to allow the imaging agent to bind selectively to specific sites such as receptors on tumor cells to improve detection. For example, there are a number of cell surface receptors that are known to be overexpressed on prostatic cancer cells, including epidermal growth factor receptor (EGFR) and the laminin receptor VLA-6 (Bonkhoff et al., 1993). For a non-specific targeting, it has been shown (Duncan et al., 1998) that appropriately sized dendrimers and dendrimer-based metal complexes (e.g., *cis*-platinum) become trapped in tumor vasculature due to the *enhanced permeability* and *retention* (EPR) effect (Muggia, 1999).

Experimental

Materials. Amine terminated PAMAM dendrimers were purchased from Dendritech and were dialized before use. All other reagents were purchased from the Aldrich Chemical Co., and were used as received. Positively charged $\{(Au(0)_{10}$-PAMAM_E5·$NH_2\}$ gold-dendrimer complexes (theoretical particle mass = 30,830 D, calculated as the average mass of nanocomposite units composed of the template and the encapsulated gold atoms) were prepared by mixing dilute solutions of generation five PAMAM dendrimer (128 primary amine termini) with a dilute solution of $HAuCl_4$. In the first step, a salt formed between the tertiary nitrogen branching centers of the dendrimer and the tetrachloroaurate anions (Balogh et al., 1999; Esumi et al., 2000; Gröhn et al., 2000). The reduction was completed by irradiating the sample with light (Esumi et al., 1998). DNC solutions were deep red indicating reduction of the complex salts into metallic gold and the formation of a nanocomposite structure. The starting materials and the obtained products were carefully characterized by UV-vis, ^{1}H and ^{13}C NMR spectroscopy, size exclusion chromatography (SEC) and high resolution transmission electron microscopy (HRTEM). Details of the experimental procedure and analytical techniques can be found in a previous study (Balogh et al., 1999).

Instrumentation. IR spectra were recorded on a Nicolet 20DBX FT-IR spectrophotometer between CaF_2 plates, UV-visible spectra were obtained on a Cary 1E spectrophotometer at room temperature between 200 and 900 nm in a Suprasil 300 quartz cell (L = 1 mm). ^{1}H and ^{13}C NMR measurements were carried out by a Varian Unity 300 multinuclear spectrometer equipped with a temperature controller. SEC was performed on three TSK gel columns (4000, 3000 and 2000) using a Waters 510 pump with a Wyatt Technology Dawn DSP-F MALLS and Wyatt Technology 903 interferometric refractometer and a Waters 510 pump with a Waters 410 differential refractometer respectively. A Phillips EM301 instrument was applied for TEM using Formvar

coated carbon grids. Image analysis was performed on a Macintosh computer using the public domain NIH Image program (developed at the US National Institutes of Health and available on the Internet at http://rsb.info.nih.gov/nih-image/).

Results and discussion

We have investigated the behavior of gold/PAMAM dendrimer nanocomposites under various biologic conditions. In imaging, gold nanocomposites offer the high electron density of the immobilized gold atoms, while the interactions of the gold atomic domains with the surrounding biologic environment are determined by the surface of the nanocomposite. In the case of $\{Au(0)\}_1$, an internal nanocomposite, the surface of the composite particle is controlled by the host dendrimer. Thus, interaction of the host with the biological environment can be controlled by increasing or decreasing the number and/or strength of interacting forces on the dendrimer surface area by changing the number and character of the surface groups.

Imaging of {Au} gold nanocomposites in vitro *and* in vivo

A few atoms of gold per PAMAM dendrimer already make possible the visualization of the amorphous single and multiple nanocomposite units both in tissues and in cells by electron microscopy. A typical HRTEM image of a positively charged $\{Au(0)_{7.5}$-PAMAM_E5·$NH_2\}$ is shown in Figure 4. The size distribution tends to be uniform and centered around, although an extensive amount of aggregation may occur on the carbon coated TEM grid similar to those observed in the literature (Esumi et al., 2000; Gröhn et al., 2000).

Due to the synthetic procedure used $\{(Au(0)_n\}_m$ clusters are almost always present in the solution of $\{(Au(0)_n\}$ nanocomposites (He et al., 1999). Of course, visibility of the larger clusters are much better than the single units, which often appear as small grayish round objects due to their low and homogenously dispersed gold content.

This characteristic size (5 and 25 nm), shape (spherical) and strong TEM contrast make the observation of gold nanocomposites simple by electron microscopy. Furthermore, no other objects can be found in tissues or cells that are similar in shape, size and especially contrast to the gold nanocomposite clusters.

DNCs can have a specific charge on their host polymer and therefore may be used to map certain cell compartments and cellular structures. These local interactions may be induced by either charge or surface (p_H or protein content). Interacting cellular structures that are preferred by various nano-particles can be made visible this way. These local interactions may be induced by either charge or surface (p_H or protein content). Charged and hydrophilic $\{Au\}$ nanocomposites does not stain the hydrophobic areas of the specimen, but those structures that bind various nanocomposites by various interactions are easily observed.

In the HRTEM image of $\{Au(0)_{7.5}$-PAMAM_E5·$NH_2\}$, the habit planes formed by the small gold domains within the connecting dendrimer nanocomposite single units are apparent (Figure 5). The diameter of the dendrimer template is about 5 nm and the observed nanoparticles are between 5 and 10 nm, which

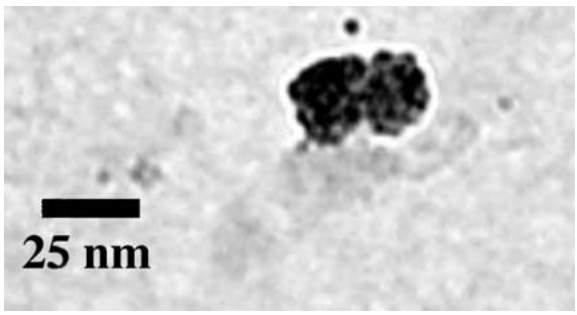

Figure 4. Comparison of a single $\{(Au(0)_n$-E5·$NH_2\}$ particle and a $(\{Au\}_n)_2$ a dimer of nanocomposite clusters.

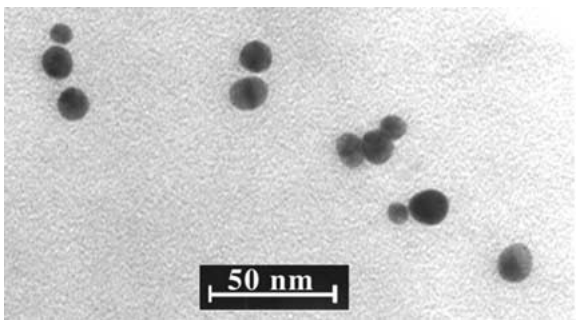

Figure 5. TEM of the particular gold nanocomposite used in the experiment described in the text. Single nanocomposite units appear as grayish round objects while small clusters display straight lines due to the higher local concentration of gold in the connecting planes.

is consistent with the dendrimer size measured by TEM and also with the other references (Jackson et al., 1998).

Transfection and visualization of intracellular trafficking of dendrimers

Due to the metal content, the cellular uptake and trafficking of {Au} nanocomposites and their DNA complexes can be simultaneously observed using electron microscopy.

We have used reporter plasmid DNA and positively charged gold $\{Au(0)_n$-PAMAM$\}$ nanocomposites to visualize the intracellular trafficking of DNA/PAMAM dendrimer complexes. Complexes of plasmid DNA (pCF1/LUC; 5.5 kb) and gold nanocomposites of $\{Au(0)_{10}$-PAMAM_E5·$NH_2\}$ were formed in double distilled H_2O at a 10 : 1 ({Au} : pDNA) charge ratios, which represent the typical condition of complex formation. Gene transfections were performed by incubating the complexes with Cos-1 cells (monkey kidney fibroblasts; 1×10^5 cells/cm^3) for 3 h at 37°C. Cells were washed and grown overnight (24 h, 37°C) in growth medium supplemented with 10% FBS.

The luciferase expression was found comparable to that in the control transfections performed by using regular PAMAM_E5·NH_2 (Figure 6). This indicated that presence of metal component in the {Au} nanocomposite does not inhibit processes of transfer, subsequent transcription and translation of the introduced DNA. We have not observed any increase in toxicity due to the metal content of gold nanocomposites indicating that toxicity of these nanomaterials is determined by the dendrimer used.

To examine {Au} localization by TEM, Jurkat cells were fixed at 4°C in 2.5% glutaraldehyde and post-fixed in 1% osmium tetroxide. Selected samples were *en bloc* stained with 3% uranyl acetate. Ultra-thin sections were examined on a Philips CM100 TEM.

$\{Au\}_n$ clusters appear as 25–30 nm dark spots while $\{Au\}^+$ positively charged single gold/dendrimer nanocomposites interacting with several pDNA molecules that result in the gray stain of the complex. Only multiple pDNA/$\{Au\}^+$ complexes were observed under the experimental conditions we used. Initially these complexes were found attached to the cell surface. Then, they were subsequently endocytosed and they entered lysosomal compartment of cells. Figure 7 illustrates all these three steps.

Interestingly, the original distribution of the highly visible $\{Au\}_n$ clusters is clearly random in the pDNA-{Au} complexes. However, images taken at a later time indicate the movement of the dark nanoparticles toward the internal surface of the lysozomal vesicles indicating flow characteristic of a living cell (Figure 8).

Conclusions

TEM imaging of gold/PAMAM dendrimer nanocomposites in the 5–25 nm range was demonstrated including *in vitro* and *in vivo* conditions. These gold

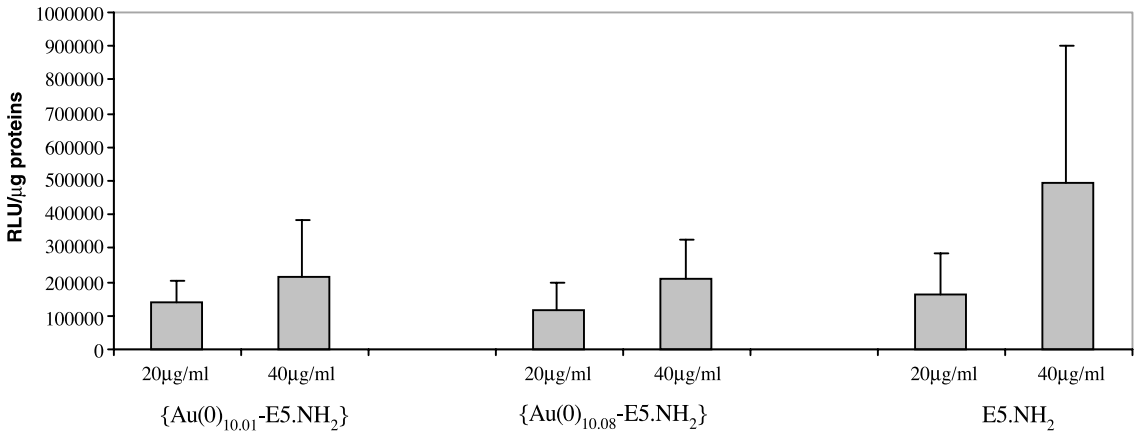

Figure 6. In vitro transfection using PAMAM dendrimers and their gold nanocomposites. Two independent preparations of $\{Au(0)_n$-PAMAM_E5·$NH_2\}$ nanocomposites containing $n = 10.01$ and $n = 10.09$ gold atoms per dendrimer on average were compared with the transfection using the parent dendrimer. The efficiency of transfection was measured as luciferase protein expression standardized to protein content in the cell lysate.

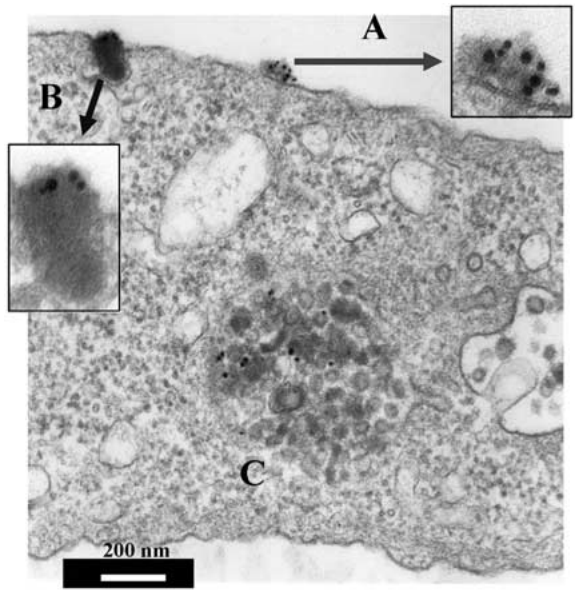

Figure 7. Visualization of gene transfection with plasmid DNA-gold/PAMAM nanocomposite complex aggregates. A: Cell surface attachment, B: Complex aggregate just undergoing endocytosis, C: Complexes localized in lysozome.

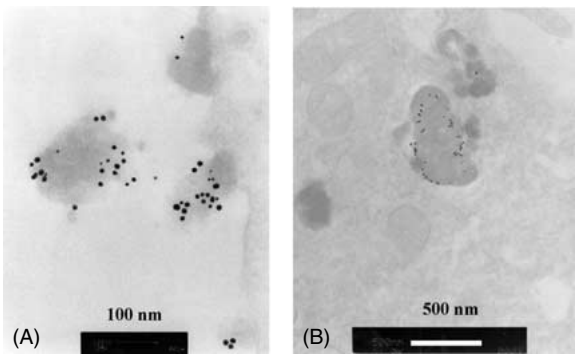

Figure 8. (A) Random distribution of $\{Au\}_n$ nanocomposite clusters before and during cell surface attachment, and (B) localized near the internal membrane of the lysozome after approximately 4 h.

nanocomposites are easy to observe in cells and in tissue because they are very much differ by contrast, size and shape, while they preserve the properties of the organic dendrimer templates. As an example, the internalization of pDNA/dendrimer complexes were made visible by TEM using a gold nanocomposite instead of a dendrimer. Positively charged gold/PAMAM nanocomposites used as DNA carriers were capable of gene transfection with efficiencies similar to their host dendrimer. It appears that in contrast to general beliefs, in this gene transfection process large pDNA-PAMAM clusters form (containing many DNA molecules and many dendrimers) which then undergo endocytosis after surface binding. Another example was the case of lipid bilayers, where the positively charged gold/dendrimer single nanocomposite units easily penetrated into the polar zone of the bilayer structure thereby rendering them visible by TEM.

The diffusion of various dendrimer nanocomposite is controlled rather by the polymer host than by the inorganic guests. Thus, by varying the charge and lipophilicity of the host, the particle can enter into interaction with various biologic entities. Using radioactive gold as a guest, the nanoscopic agent can be directly injected into the tumor microvasculature. Positively charged DNCs rapidly accumulated in the nucleus of the tumor cell.

Acknowledgements

This project has been funded with Federal funds in part from the U.S. Department of Energy, under Award No. FG01-00NE22943, in part from the National Cancer Institute, National Institutes of Health, under Contract No. NO1-CO-97111 and in part by the Defense Advanced Research Projects Agency, award MDA972-97-1-0007, entitled 'Nanomolecule Based Agents for Pathogen Counter Measure'.

References

Balogh L., R. Valluzzi, K.S. Laverdure, S.P. Gido, G.L. Hagnauer & D.A. Tomalia, 1999. J. Nanopart. Res. 1(3), 353.

Balogh L., D.R. Swanson, R. Spindler & D.A. Tomalia, 1997. Formation and characterization of dendrimer-based water soluble inorganic nanocomposites. Proceedings of ACS PMSE (77), 118.

Beck Tan N., L. Balogh & S. Trevino, 1997. Structure of metallo-organic nanocomposites produced from dendrimer complexes. Proceedings of ACS PMSE (77), 120.

Bhalgat M.K. & J.C. Roberts, 2000. Eur. Polym. J. 36(3), 647–651.

Bielinska A.U., J.F. Kukowska-Latallo, J. Johnson, D.A. Tomalia & J.R. Baker, Jr., 1996. Nucleic Acids Res. 24, 2176.

Bielinska A.U., J.F. Kukowska-Latallo & J.R. Baker, Jr., 1997. Biochim. Biophys. Acta 1353(2), 180.

Bielinska A.U., C. Chen, J. Johnson & J.R. Baker, Jr., 1999. Bioconjug. Chem. 10, 843–850.

Bonkhoff H. et al., 1993. Hum. Pathol. 24, 243–248.

Chen W., N.J. Turro & D.A. Tomalia, 2000. Langmuir 16, 15.

de Gennes P.G. & H. Hervet, 1983. J. Phys. Lett. (Paris) 44(9), 351.
Duncan R. et al., 1998. Polym. Prep., Am. Chem. Soc. Div. Polym. Chem. 39, 180.
Esumi K., A. Suzuki, N. Aihara, K. Usui & K. Torigoe, 1998. Langmuir 14(12), 3157.
Esumi K., A. Suzuki, A. Yamahira & K. Torigoe, 2000. Langmuir 16, 2604.
Garcia M.E., L.A. Baker & R.M. Crooks, 1999. Anal. Chem. 71, 256.
Gröhn F., B.J. Bauer, Y.A. Akpalu, C.L. Jackson & E.J. Amis, 2000. Macromolecules 33(16), 6042.
Hawker C.J. & J.M.J. Frechet, 1990. J. Am. Chem. Soc. 112, 7638.
He J.-A., R. Valluzzi, K. Yang, T. Dolukhanyan, C.M. Sung, J. Kumar, S.K. Tripathy, L. Samuelson, L. Balogh & D.A. Tomalia, 1999. Chem. Mater. 11, 3268.
Jackson C.L., H.D. Chanzy, F.P. Booy, B.J. Drake, D.A. Tomalia, B.J. Bauer & E.J. Amis, 1998. Macromolecules 31, 6259–6265.
Kim Y.K. & S.C. Zimmerman, 1998. Curr. Opin. Chem. Biol. 2(6), 733–742.
Kobayashi H., N. Sato, S. Kawamoto, T. Saga, A. Hiraga, T.L. Haque, T. Ishimori, J. Konishi, K. Togashi & M.W. Brechbiel, 2001. Bioconjug. Chem. 12, 100–107.
Kukowska-Latallo J.F., A.U. Bielinska, J. Johnson, R. Spindler, D.A. Tomalia & J.R. Baker, Jr., 1996. Proc. Natl. Acad. Sci. 93, 4897.
Mansfield M.L. & L.I. Klushin, 1993. Macromolecules 26, 4262.
Margerum L.D., B.K. Campion, M. Koo, N. Shargill, J. Lai, A. Marumoto & P.C. Sontum, 1997. J. Alloys Compd. 249(1–2), 185.
Muggia F.M., 1999. Clin. Cancer Res. 5, 7.
Newkome G.R., Z.-Q. Yao, G.R. Baker & V.K. Gupta, 1985. J. Org. Chem. 50, 2003.
Ottaviani M.F., B. Sacchi, N.J. Turro, W. Chen, S. Jockusch & D.A. Tomalia, 1999. Macromolecules 32, 2275.
Qin L., D.R. Pahud, Y. Ding, A.U. Bielinska, J.F. Kukowska-Latallo, J.R. Baker Jr., & J.S. Bromberg, 1998. Hum. Gene Ther. 9(4), 553–560.
Roessler B.J., A.U. Bielinska, K. Janczak, I. Lee & J.R. Baker Jr., 2001. Biochem. Biophys. Commun. 283, 124–129.
D.A. Tomalia, J.R. Dewald, M.J. Hall, S.J. Martin & P.B. Smith, 1984. First SPSJ Int. Polym. Conference, Kyoto, Japan, August, 65.
Tomalia D.A., H. Baker, J. Dewald, M. Hall, M. Kallos, S. Martin, J. Roeck, J. Ryder & P. Smith, 1985. Polym. J. (Tokyo) 17, 117–132.
Tomalia D.A. & P. Dvornic, 1996. In: Salamone J.C. ed. Polymeric Materials Encyclopedia. Vol. 3(D–E) CRC Press, p. 1814.
Tomalia D.A., A.M. Naylor & W.A. Goddard III, 1990. Angew. Chem. Int. Ed. Engl. 29, 138.
Wilbur D.S. et al., 1998. Bioconjug. Chem. 9, 813–825.
Wu C., M.W. Brechbiel, R.W. Kozak & O.A. Gansow, 1994. Bioorg. Med. Chem. Lett. 4(3), 449.